UNSTEADY MHD FLOW OF RADIATING CASSON FLUID THROUGH A PERMEABLE CHANNEL WITH SLIP, BUOYANCY FORCE AND HEAT SOURCE

OM PRAKASH†, O.D. MAKINDE‡ and R.L. MONALEDI‡

† *School of Basic and Applied Sciences, Galgotias University Greater Noida, Uttar Pradesh, India*
Corresponding author: op_ibs@rediffmail.com
‡ *Faculty of Military Science, Stellenbosch University Private Bag X2, Saldanha 7395, South Africa.*

***Abstract*— Analytical investigation is performed into an unsteady Magnetohrodynamics mixed convective Casson fluid flow and heat transfer characteristics with thermal radiation, wall slip, heat source and buoyancy force in a permeable vertical channel. The fluid is injected into the left wall of the channel and sucked out at right wall. The governing momentum and energy balance equations are achieved and tackled analytically. The effects of numerous thermophysical parameters on the temperature profiles, velocity, Nusselt number as well as skin friction are presented graphically and discussed qualitatively. The results show that a temporal decline in both the fluid temperature and velocity profiles with thermal buoyancy. Moreover, the enhancement in heat transfer due to wall injection/suction also causes the skin friction to decrease.**

***Keywords*— Unsteady channel flow; MHD Casson fluid; Velocity slip; Buoyancy force; Radiative heat.**

I. INTRODUCTION

Hydromagnetic flows of Non-Newtonian fluids have numerous utilizations in industry as well as engineering. These include refinement of crude oil, magnetohydrodynamics generators, plasma studies, nuclear reactors liquid metal, geothermal energy extraction, etc. (Cramer and and Pai, 1973; Abel *et al.*, 2005). Due to complexity of non-Newtonian fluids behavior, no single constitutive equation can be utilized to describe all the non-Newtonian fluid properties. However, numerous models of Non-Newtonian fluids have been proposed in the literature base on integral, differential and rate type categories. One of such non-Newtonian model is the Casson fluid model (Casson, 1959). A Casson fluid is a plastic fluid which exhibits yield stress in its constitutive equation. There are so many illustrations of Casson fluid flow model like jelly, synovial fluids, tomato sauce, concentrated fruit juices, honey, food processing, soup, drilling operations coal in water, synthetic lubricants, metallurgy, paints, sewage sludge manufacturing of pharmaceutical products and various more. Human blood is also assumed to be Casson fluid due to the existence of various materials like, fibrinogen, globin and protein in aqueous base plasma in the blood. Hence, the Casson fluid applications can be found in engineering, industrial processes, pharmaceutical, food technology, polymer production, aerospace technology and numerous hospital treatments.

Several researchers have investigated Casson fluid flow with heat transfer under various physical situations and configurations. Joye (2003) analyzed cylindrical geometries for viscosity and shear rate corrections for a Casson fluid. Attia and Sayed-Ahmed (2012) analyzed the behavior of MHD Couette flow for a Casson fluid with heat transfer between parallel plates. Mustafa *et al*. (2011) analyzed the unsteady flow behavior for Casson fluid past a moving flat plate in presence of heat transfer. Mukhopadhyay (2013) analyzed the transient flow of a Casson fluid with heat transfer over a stretching surface with suction/blowing and observe that due to an enhancement in Casson parameter the velocity field is vanquished and thermal diffusivity and the temperature are increased due to enhancement in thermal radiation. Pramanik (2014) proposed a Casson fluid model for boundary layer flow of a non-Newtonian fluid in presence of heat transfer as well as suction or blowing at the surface. Rao *et al*. (2015) described the nature of Casson non-Newtonian fluid with of heat transfer and hydrodynamic slip conditions under a semi-infinite vertical plate for laminar boundary layer flow. Sekhar *et al*. (2015) considered the effects of diffusion thermo on transient combined convection magneto hydrodynamics boundary layer flow in presence of porous medium for Casson fluid. Pushpalatha *et al*. (2016) proposed a Casson fluid model under convective boundary conditions for transient free convection flow for a channel bounded by a moving vertical flat plate in a rotating system. The influence of nonlinear thermal radiation and magnetic field on Casson fluid flow over a cone under chemical reaction were elaborate by Raju and Sandeep (2016). Bala and Reddy (2016) discussed the combined effect of chemical reaction and thermal radiation on a Casson fluid on an exponentially inclined permeable stretching surface. Benazir *et al.* (2016) presented a model for hydromagnetic Casson fluid flow with non-uniform heat source/sink on a a vertical cone and flat plate in presence of porous medium. The effects of magnetic fields on heat transfer and stagnation point flow on Casson Nano-fluid over a stretching sheet with slip and convective boundary condition were discussed by Ibrahim and Makinde (2016). Surzhikov and Shang (2004) proposed a two-component plasma model for two-dimensional glow discharge in presence of magnetic field. The appropriateness of hydrodynamic characterization for plasma flow in the heliospheric interface is discussed by Baranov and Ruderman (2013). The problem of decomposition of methane hydrate coexisting with water in a high permeability reservoir is considered by Tsypkin (2017). Heat and porous medium effects on MHD flow have been discussed by various authors (Prakash and Makinde, 2015; Ahmed and Batin, 2014; Makinde, 2011; Das, 2017).

From the literature survey, it implies that the problem of unsteady flow of a conducting Casson fluid with heat transfer in a permeable channel under the influence of wall slip, thermal radiation, heat source, buoyancy force and magnetic field has not received too much consideration of researchers.

In this paper, we study joint effects of thermal radiation, heat source, buoyancy force, wall slip and magnetic field on unsteady flow of a conducting Casson fluid through a permeable channel. In the given sections, the model problem is designed and solved analytically. Obtained results are discussed quantitatively and represented graphically.

II. PROBLEM FORMULATION

We examine the unsteady hydromagnetic mixed convective flow of an electrically conducting radiating Casson fluid in a vertical channel with permeable walls placed at $y=0$ and $y=L$ as shown in Fig. 1. The flow is considered with a uniform transverse magnetic field of amount B_0 which applied perpendicular to channel, the induced electric fields are considered to be very small and the magnetic Reynolds number is negligible. In addition, fluid injection takes place at the channel left wall, while suction is taking place at the right wall. The channel left wall is kept at temperature T_0 while the right wall is maintained at temperature T_1 such that $T_0 \leq T_1$.

Taking into account the hypothesis made above, the governing equations under the usual Boussinesq approximation are given in the following form

$$\frac{\partial u}{\partial \tau}+V\frac{\partial u}{\partial y}=-\frac{1}{\rho}\frac{\partial p}{\partial x}+\upsilon\left(1+\frac{1}{\gamma}\right)\frac{\partial^2 u}{\partial y^2}-\frac{\sigma B_0^2 u}{\rho}+\beta g(T-T_0) \quad (1)$$

$$\rho c_p\left(\frac{\partial T}{\partial \tau}+V\frac{\partial T}{\partial y}\right)=k\frac{\partial^2 T}{\partial y^2}-\frac{\partial q_r}{\partial y}+Q(T-T_0) \quad (2)$$

where u, p, T, σ, ρ, υ, k, c_p, Q, τ, g, β, γ and V are respectively, the fluid velocity in x-direction, pressure, fluid temperature, fluid electrical conductivity, fluid density, kinematic viscosity, thermal conductivity coefficient, specific heat at constant pressure, the heat source parameter, time, gravitational acceleration, thermal expansion coefficient, the Casson parameter and the wall suction / injection velocity. With the help of Rosseland approximation for thermal radiation in optically thick media, theradiative heat flux q_r is given by Rosseland (1936) and Brewster (1992).

$$q_r=-\frac{4\sigma^*}{3k^*}\frac{\partial T^4}{\partial y}\approx-\frac{16\sigma^* T_0^3}{3k^*}\frac{\partial T}{\partial y} \quad (3)$$

where σ^* is the Stefan–Boltzman constant and k^* is the mean absorption coefficient. The expression in Eq. (3) is obtained by considering that the temperature differences between the fluid and the channel walls are enough small and $T^4 \approx 4TT_0^3-3T_0^4$. The appropriate initial and boundary conditions for the temperature and fluid velocities are described below:

$$u(y,0)=F(y), T(y,0)=H(y) \quad (4)$$
$$u(0,\tau)=0, T(0,\tau)=T_0$$
$$u(L,\tau)=-b\left(1+\frac{1}{\gamma}\right)\frac{\partial u}{\partial y}(L,\tau), T(L,\tau)=T_0(1+e^{-\alpha\tau})$$

where α is the frequency parameter and b is the slip length parameter. Dimensionless variables and parameters are given below:

$$\eta=\frac{y}{L}, \theta=\frac{T-T_0}{T_0}, t=\frac{\tau\upsilon}{L^2}, \upsilon=\frac{\mu}{\rho}, \lambda=\frac{\alpha L^2}{\upsilon}, \quad (5)$$
$$Nr=\frac{16\sigma^* T_0^3}{3kk^*}, \mathrm{Re}=\frac{VL}{\upsilon}, \mathrm{Pr}=\frac{\mu c_p}{k}, \delta=\frac{b}{L}, X=\frac{x}{L},$$
$$M=\frac{\sigma B_0^2 L^2}{\mu}, \bar{p}=\frac{L^2 P}{\rho\upsilon^2}, Gr=\frac{\beta g T_0 L^3}{\upsilon^2}, S=\frac{QL^2}{\rho c_p \upsilon}$$

Putting Eq. (5) into Eqs. (1)-(4), we achieve,

$$\frac{\partial U}{\partial t}+\mathrm{Re}\frac{\partial U}{\partial \eta}=-\frac{\partial \bar{p}}{\partial X}+\left(1+\frac{1}{\gamma}\right)\frac{\partial^2 U}{\partial \eta^2}-MU+Gr\theta, \quad (6)$$

$$\frac{\partial \theta}{\partial t}+\mathrm{Re}\frac{\partial \theta}{\partial \eta}=\left(\frac{1+Nr}{\mathrm{Pr}}\right)\frac{\partial^2 \theta}{\partial \eta^2}-S\theta, \quad (7)$$

with

$$U(\eta,0)=F(\eta), \theta(\eta,0)=H(\eta) \quad (8)$$
$$U(0,t)=0, U(1,t)=-\delta\left(1+\frac{1}{\gamma}\right)\frac{\partial U}{\partial \eta}(1,t)$$
$$\theta(0,t)=0, \theta(1,t)=e^{-\lambda t},$$

where Pr is the Prandtl number, δ is the velocity-slip parameter, Re is suction/injection Reynolds number, Gr is the Grashof number, M is the magnetic field parameter, S is the heat source parameter, Nr is the thermal radiation parameter and λ is the wall temperature decay parameter. Other quantities of concern are Nusselt number (Nu) and skin friction coefficients (C_f) which are given as

$$C_f=\frac{L^2\tau_w}{\rho\upsilon^2}=\left(1+\frac{1}{\gamma}\right)\frac{\partial U}{\partial \eta}\bigg|_{\eta=0,1}, \quad (9)$$
$$Nu=\frac{Lq_w}{kT_0}=-(1+Nr)\frac{\partial \theta}{\partial \eta}\bigg|_{\eta=0,1},$$

where the wall shear stress τ_w and the wall heat flux q_w are given as

$$\tau_w=\mu\left(1+\frac{1}{\gamma}\right)\frac{\partial u}{\partial y}\bigg|_{y=0,L}, \quad (10)$$
$$q_w=-k\left(1+\frac{16\sigma^* T_\infty^3}{3kk^*}\right)\frac{\partial T}{\partial y}\bigg|_{y=0,L},$$

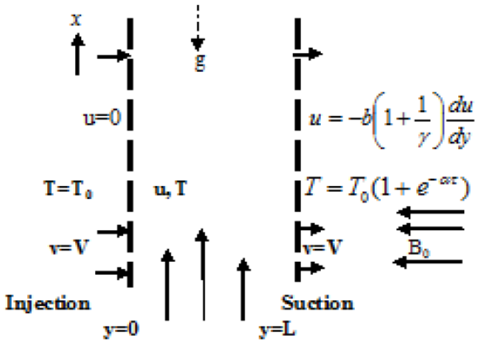

Figure 1: Schematic diagram of problem

III. METHOD OF SOLUTION

In accordance to solve Eqs. (6)-(8) analytically, we employ separation of variable technique.

Let

$$-\frac{\partial \bar{p}}{\partial X}=Ae^{-\lambda t}, U(\eta,t)=F(\eta)e^{-\lambda t}, \quad (11)$$
$$\theta(\eta,t)=H(\eta)e^{-\lambda t}$$

Putting Eq. (11) into Eqs. (6)-(8), we get

$$\left(1+\frac{1}{\gamma}\right)\frac{d^2F}{d\eta^2}-\mathrm{Re}\frac{dF}{\partial\eta}+(\lambda-M)F=-A-GrH, \quad (12)$$

$$\left(\frac{1+Nr}{\mathrm{Pr}}\right)\frac{d^2H}{d\eta^2}-\mathrm{Re}\frac{dH}{\partial\eta}+(\lambda+S)H=0, \quad (13)$$

$$F(0)=0, H(0)=0, \quad (14)$$

$$F(1)=-\delta\left(1+\frac{1}{\gamma}\right)\frac{dF}{d\eta}(1),\ \ H(1)=1,$$

Equations (12)-(14) are tackles analytically and we obtained the following solutions for the temperature as well as velocity profiles:

$$\theta(\eta,t)=\left(\frac{1}{e^{r_1}-e^{r_2}}\right)[e^{r_1\eta}-e^{r_2\eta}]e^{-\lambda t} \quad (15)$$

Using MAPLE, the non-homogeneous model Eq. (12) is solved for the velocity profile as shown in the appendix. The expression for Nusselt number as well as skin friction at the channel walls are obtained from Eq. (9) as:

$$Cf|_{\eta=0}=\left(1+\frac{1}{\gamma}\right)[z_{12}B_1+z_{11}B_2-A_{12}r_1+A_{13}r_2]e^{-\lambda t}$$

$$Cf|_{\eta=1}=\left(1+\frac{1}{\gamma}\right)[z_{12}B_1e^{B_1}+z_{11}B_2e^{B_2}-A_{12}r_1e^{r_1}+A_{13}r_2e^{r_2}]e^{-\lambda t}$$

$$Nu=-\left(\frac{d\theta}{d\eta}\right)_{\eta=0}=-\left(\frac{1}{e^{r_1}-e^{r_2}}\right)[r_1-r_2]e^{-\lambda t}$$

$$Nu=-\left(\frac{d\theta}{d\eta}\right)_{\eta=1}=-\left(\frac{1}{e^{r_1}-e^{r_2}}\right)[r_1e^{r_1}-r_2e^{r_2}]e^{-\lambda t}$$

IV. RESULTS AND DISCUSSIONS

In order to investigate the influence of the emerging parameters on the thermal and flow structure of a conducting Casson fluid under consideration, the numerical computation of the analytical solutions obtained are performed and presented in Figs. 2-17. In most of our computations, we have taken $A=1$, $\mathrm{Pr}=7.1$ (i.e. water) and $Gr>0$ (i.e. cooling), $\mathrm{Re}>0$ (i.e. injection at the left surface and suction at the right surface of channel) and $S>0$ (i.e. heat source).

A. Velocity Profiles

Figures (2)-(9) depict the velocity profiles in transverse direction. Generally, the fluid velocity is zero at the left wall, gaining to its pick value within the channel and reduces to a value at the right wall due to slip. It is noteworthy that the velocity profiles tend to skew against the right surface due to suction. In Fig. 2, it is found that the Casson fluid velocity temporally reduces. This can be attributed to the increasing cooling effects at the right wall with time. In Figs. (3) -(5), an enhancement in Re, M and Pr, causes a loss in the velocity profiles. As both fluid injection at the left as well as suction at the right surfaces increases, the cross flow velocity tends to dominate the flow regime, leading to a loss in the axial velocity profile. Moreover, the existence of magnetic field and consequently the Lorentz force in the flow regime inhibits the axial velocity profile. Increase in Prandtl number corresponds to a gain in the fluid viscosity and a loss in the thermal diffusivity, consequently, the fluid velocity decreases. Figures (6)-(9) reveal a loss in the fluid velocity as the parameter values of δ, S, Gr and γ increase. This can be attributing to the joint consequences of wall slip, heat source, thermal buoyancy and the Casson fluid yield stress. The presence of slip at the right surface of channel tends to enhance the axial motion of the fluid. In addition, the fluid converted to thin and flow speedy with upturning temperature because to heat source thermal buoyancy effects. Meanwhile, as the Casson parameter increases, the plastic fluid behavior changes gradually into that of

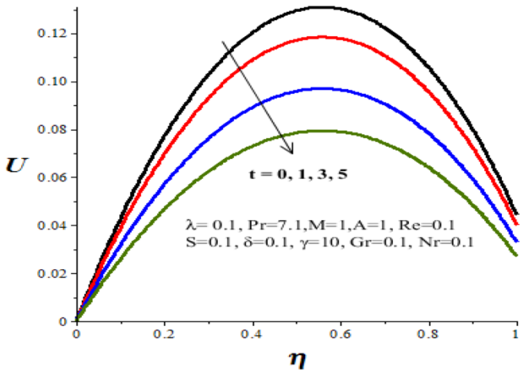

Figure 2: Velocity profiles for increasing time

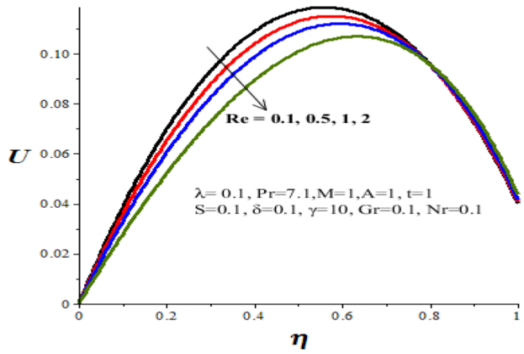

Figure 3: Velocity profiles for increasing injection/suction Reynolds number Re.

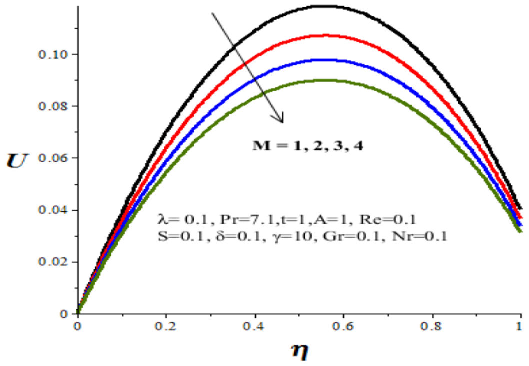

Figure 4: Velocity profiles for increasing magnetic field parameter M.

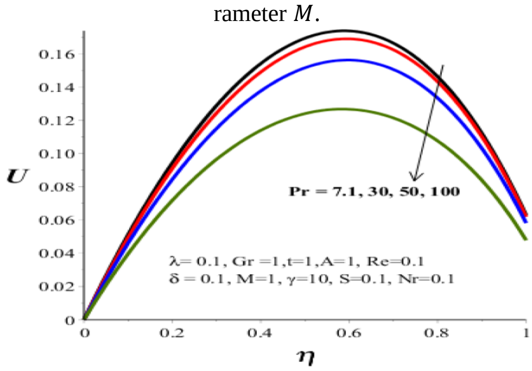

Figure 5: Velocity profiles for increasing Prandtl number Pr.

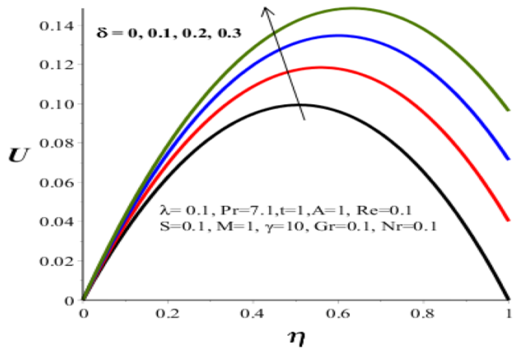

Figure 6: Velocity profiles for increasing slip parameter δ.

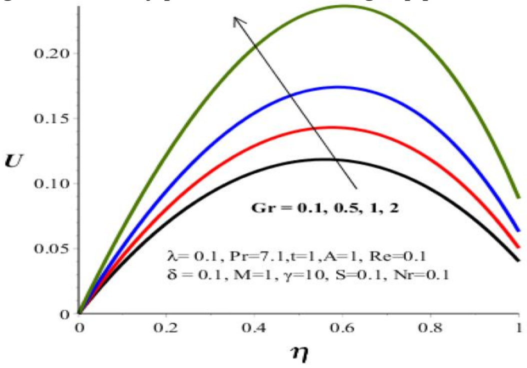

Figure 7: Velocity profiles for increasing Grashof number Gr.

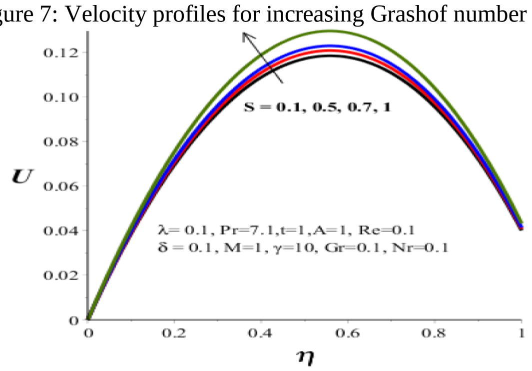

Figure 8: Velocity profiles for increasing heat source parameter S.

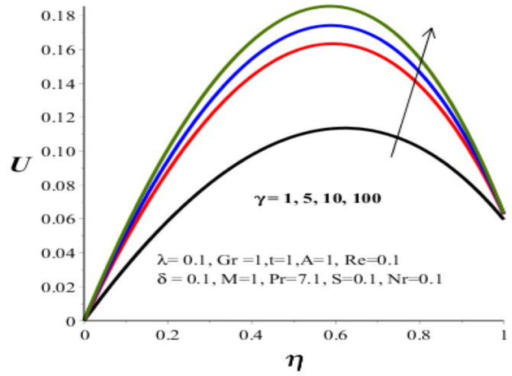

Figure 9: Velocity profiles for increasing Casson parameter γ.

Newtonian fluid regime, results to an improvement in the velocity profile.

B. Temperature Profiles

The influences of parameter variation on temperature profiles are displayed in Figs. (10)-(13). Normally, the fluid temperature is minimum at the left surface of channel, then growing to the prescribed amount at the right

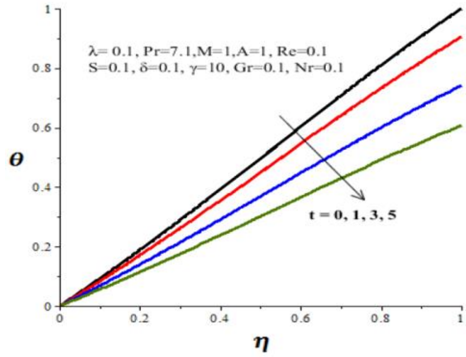

Figure 10: Temperature profiles for increasing time t.

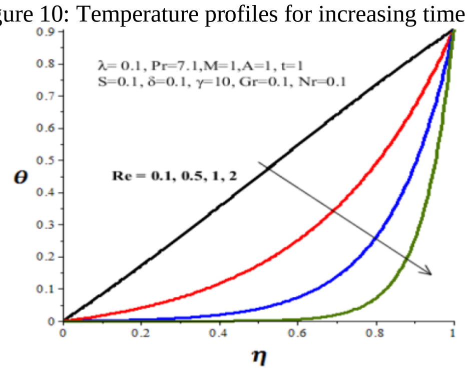

Figure 11: Temperature profiles for increasing injection/suction Reynolds number Re.

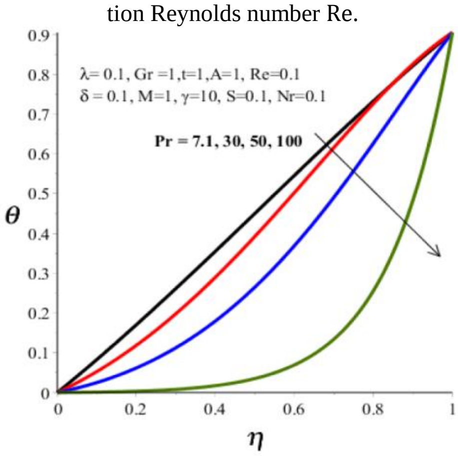

Figure 12: Temperature profiles for increasing Prandtl number Pr.

wall. In Fig. (10), it is remarkable that the Casson fluid temperature reduces with time. This can be associated to the imposed temporal cooling effect at the right surface of the channel. In Figs. (11)-(12), a hike in Re and Pr, causes a decrease in temperature profiles. The fluid suction at the right wall enhances heat loss to the ambient dominating to a decrease in temperature. Moreover, as the Prandtl number boosts, the thermal diffusivity decreases with high fluid viscosity, therefore, the fluid temperature reduces. It is also significant to mark that the temperature profiles lead to skew against the right surface of channel due to suction. Interestingly, the fluid temperature boosts to its pick value within the channel and then decrease to the prescribed right wall value with a rise in the heat source as shown in Fig. (13). This is expected, since the presence of external heat source provides addition heating of the fluid causing an elevation in the temperature profile.

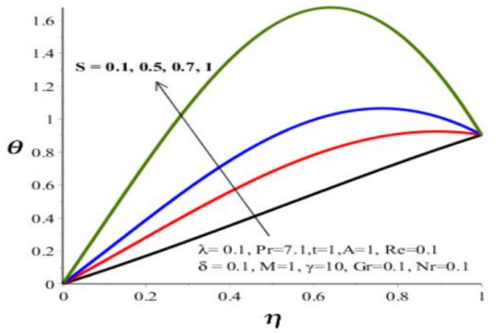

Figure 13: Temperature profiles for increasing heat source parameter S.

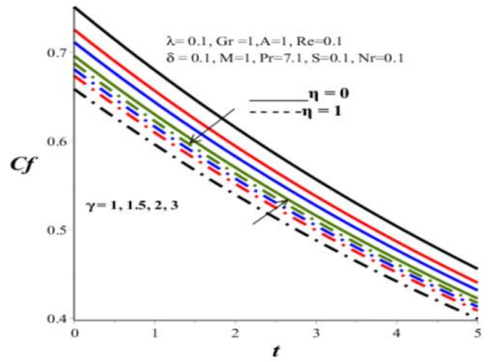

Figure 14: Skin friction for increasing time t.

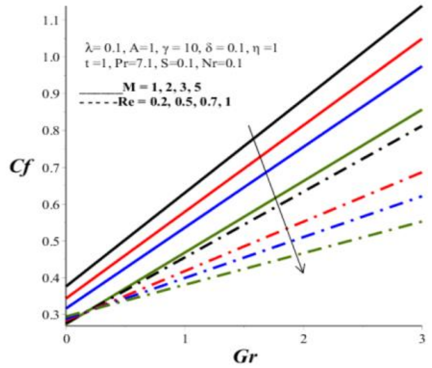

Figure 15: Skin friction for increasing Gr, M and Re.

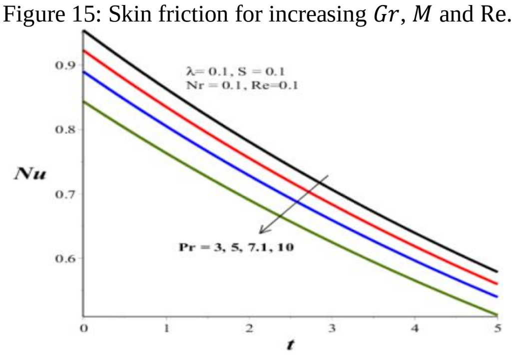

Figure 16: Nusselt number for increasing Prandtl number Pr.

C. Skin Friction and Nusselt Number

Figures (14) -(17) describes the consequences of thermophysical parameters on the Nusselt number and skin friction. Normally, the skin friction is greater at the left surface of channel as compare to the one at the right surface. This may be associated to the presence of slip at the right surface that tends to diminish the effect of wall shear-stress. Meanwhile, it is curious to mark that the skin friction temporally reduces due to a loss in the velocity gradient with time as shown in Fig. (14). A boost in the Casson fluid parameter accounts a loss in the left wall skin friction and a gain in the right wall skin friction. Figure (15) shows that the skin friction rises with an improvement in Gr and reduces with a boost in M and Re. This may be associated to a boost in the velocity gradient with thermal buoyancy and a loss in the fluid velocity and velocity gradient due to magnetic field and fluid injection/suction. In Fig. (16), we observed that the rate of heat transfer at the walls reduces with time and Prandtl number. Moreover, the Nusselt number boosts with an improvement in parameter values of Re and Nr but reduces with a gain in S as shown in Fig. (17). As the thermal radiation absorption and fluid injection/suction boosts, the fluid temperature gradient boosts leading to a hike in Nusselt number. However, a rise in the external heat source causes a loss in the fluid temperature gradient and consequently, Nusselt number reduces.

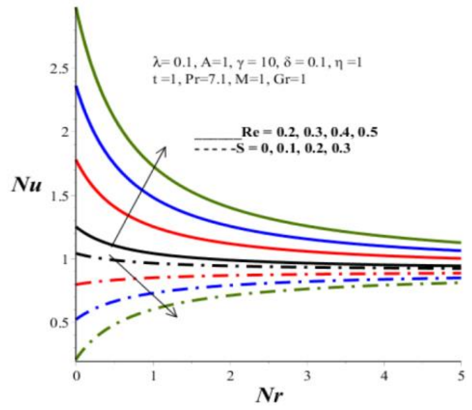

Figure 17: Nusselt number for increasing Nr, Re and S.

V. CONCLUSION

The unsteady hydromagnetic flow of a radiating Casson fluid and heat transfer through a porous vertical channel with slippery and non-uniform walls temperature was analytically examined. The effects of various emerging thermophysical parameters on the entire flow structure and the thermal putrefaction were obtained and discussed graphically and quantitatively. Our results can be summarized as follows:

- The Casson fluid temperature and velocity temporally reduces due to the time dependent cooling effects at the right surface of channel.
- Fluid velocity decreases with Re, M and Pr but increases with Gr, S, δ and γ.
- Fluid temperature decrease with Re and Pr but increases with S.
- Both Nusselt number as well as skin friction decreases with time.
- Skin friction decreases with M, Pr and Re but increases with Gr.
- Nusselt number decreases with S and Pr but increases with Re.

APPENDIX

$$m_1 = \frac{1+Nr}{\mathrm{Pr}}, m_2 = \lambda + S, m_3 = \frac{-\mathrm{Re}}{m_1}, m_4 = \frac{m_2}{m_1},$$

$$r_1 = \frac{-m_3+\sqrt{m_3^2-4m_4}}{2}, r_2 = \frac{-m_3-\sqrt{m_3^2-4m_4}}{2},$$
$$A_1 = \left(1+\frac{1}{\gamma}\right), A_2 = \lambda - M, A_3 = \frac{-\mathrm{Re}}{A_1}, A_4 = \frac{A_2}{A_1},$$
$$A_5 = \frac{A}{A_1}, A_6 = \frac{Gr}{A_1(e^{r_1}-e^{r_2})},$$
$$B_1 = \frac{-A_3+\sqrt{A_3^2-4A}}{2}, B_2 = \frac{-A_3-\sqrt{A_3^2-4A_4}}{2},$$
$$A_{11} = \frac{A_5}{A_4}, A_{12} = \frac{A_6}{r_1^2+r_1A_3+A_4}, A_{13} = \frac{A_6}{r_2^2+r_2A_3+A_4},$$
$$B_{11} = \left[1+\delta\left(1+\frac{1}{\gamma}\right)B_1\right], B_{12} = \left[1+\delta\left(1+\frac{1}{\gamma}\right)B_2\right],$$
$$B_{13} = \left[1+\delta\left(1+\frac{1}{\gamma}\right)r_1\right], B_{14} = \left[1+\delta\left(1+\frac{1}{\gamma}\right)r_2\right],$$
$$z_{11} = \frac{A_{11}(B_{11}e^{B_1}-1)}{(B_{11}e^{B_1}-B_{12}e^{B_2})} + \frac{A_{12}(B_{11}e^{B_1}-B_{13}e^{r_1})}{(B_{11}e^{B_1}-B_{12}e^{B_2})} - \frac{A_{13}(B_{11}e^{B_1}-B_{14}e^{r_2})}{(B_{11}e^{B_1}-B_{12}e^{B_2})},$$
$$z_{12} = A_{11} + A_{12} - A_{13} - z_{11}$$

REFERENCES

Abel, A.S., Prasad K.V. and Mahaboob A.(2005) Buoyancy force and thermal radiation effects in MHD boundary layer visco-elastic fluid flow over continuously moving stretching surface. *International Journal of Thermal Sciences*. **44**, 465-476.

Ahmed, S. and Batin, A. (2014) Magnetohydrodynamic Heat and Mass Transfer Flow with Induced Magnetic Field and Viscous Dissipative Effects. *Latin American Applied Research*. **44**, 9-17.

Attia, H.A. and Sayed-Ahmed M.E. (2010) Transient MHD Couette flow of a Casson fluid between parallel plates with heat transfer. *Italian J. Pure Appl. Math.* **27**, 19-38.

Bala, P. and Reddy, A. (2016) Magnetohydrodynamic flow of a Casson fluid over an exponentially inclined permeable stretching surface with thermal radiation and chemical reaction. *Ain Shams Engineering Journal,* **7**, 593–602.

Baranov, V.B. and Ruderman, M.S. (2013) On the effect of transport coefficient anisotropy on the plasma flow in heliospheric interface. *Monthly Notices of the Royal Astronomical Society.* **434**, 3202-3207.

Benazir, A.J., Sivaraj, R. and Makinde, O.D. (2016) Unsteady magnetohydrodynamic Casson fluid flow over a vertical cone and flat plate with non-uniform heat source/sink. *International Journal of Engineering Research in Africa.* **21**, 69-83.

Brewster, M.Q. (1992) *Thermal radiative transfer and properties.* John Wiley and sons Inc. New York, USA.

Casson, N. (1959) A flow equation for pigment oil suspensions of the printing ink type. *Rheology of disperse systems.* Mill, C.C. (Ed.). Pergamum press, Oxford, 84-102.

Cramer, K.R. and Pai, S.I. (1973) *Magnetofluid dynamics for engineers and applied physicists.* McGraw–Hill, New York.

Das, U.J. (2017) Heat transfer to MHD oscillatory dusty visco-elastic fluid flow in an inclined channel filled with a porous medium. *Latin American Applied Research.* **47**, 145-150.

Ibrahim, W. and Makinde, O.D. (2016) Magnetohydrodynamic stagnation point flow and heat transfer of Casson nanofluid past a stretching sheet with slip and convective boundary condition. *Journal of Aerospace Engineering.* **29**, 04015037.

Joye, D.D. (2003) Shear rate and viscosity corrections for a Casson fluid in cylindrical (Couette) geometries. *J Colloid Interface Sci*. **267**, 204-210.

Makinde, O.D. (2011) On MHD mixed convection with soret and dufour effects past a vertical plate embedded in a porous medium. *Latin American Applied Research.* **41**, 62-68.

Mukhopadhyay, S. (2013) Effects of thermal radiation on Casson fluid flow and heat transfer over an unsteady stretching surface subjected to suction/blowing. *Chin. Phys. B.* **22**, 114702.

Mustafa, M., Hayat, T., Pop, I., and Aziz, A.(2011) Unsteady boundary layer flow of a Casson fluid due to an impulsively started moving flat plate. *Heat Transfer-Asian Research*. **40**, 553-576.

Prakash, O. and Makinde, O.D. (2015) MHD oscillatory Coutte flow of dusty fluid in a channel filled with a porous medium with radiative heat and Buoyancy force. *Latin American applied research*, **45**, 181-191.

Pramanik, S. (2014) Casson fluid flow and heat transfer past an exponentially porous stretching surface in presence of thermal radiation. *Ain Shams Engrg. J.* **5**, 205-212.

Pushpalatha, K., Sugunamma, V., Ramana Reddy, J.V. and Sandeep, N. (2016) Heat and mass transfer in unsteady MHD Casson fluid flow with vonvective boundary conditions. *International Journal of Advanced Science and Technology,* **91**, 19-38.

Raju, C.S.K. and Sandeep, N. (2016) Opposing and assisting flow characteristics of radiative Casson fluid due to cone in the presence of induced magnetic field. *International Journal of Advanced Science and Technology*, **88**, 43-62.

Rao, A., Prasad, V. R., Reddy, N.B. and Beg O.A. (2015) Heat transfer in a Casson rheological fluid from a semi-infinite vertical plate with partial slip. *Heat Transfer-Asian Research.* **44,** 272-291.

Rosseland, S. (1936) *Theoretical astrophysics*. Oxford University, New York, NY, USA.

Sekhar, K.R., Krishna, C.M. and Reddy G.V. (2015) MHD convective heat and mass transfer of a Casson fluid in a boundary layer slip flow past a vertical permeable plate. *Int. J. of Trend in Res. and Development.* **2**, 205-214.

Surzhikov, S.T. and Shang, J.S. (2004) Two-component plasma model for two-dimensional glow discharge in magnetic field. *J. of Comp. Physics*. **199**, 437-464.

Tsypkin, G.G. (2017) Formation of the impermeable layer in the process of methane hydrate dissociation in porous media. *Fluid Dynamics.* **52**, 657–665.

Received October 6, 2019
Sent to Subject Editor October 10, 2019
Accepted August 27, 2020
Recommended by Subject Editor Fabio Giannetti